Comparative Analysis of Ground-Based Wind Shear Detection Radars * ‡

Mark E. Weber, Mark A. Isaminger, Cynthia Meuse
Massachusetts Institute of Technology Lincoln Laboratory
Lexington, Massachusetts 02173

Steven V. Vasiloff, Thomas Shepherd
National Severe Storms Laboratory
Norman, Oklahoma 73069

1. Introduction

Low altitude wind shear associated with thunderstorm outflows is a significant safety hazard to aircraft on final approach or takeoff from an airport. In the last two decades, twenty-one commercial air carrier accidents have been attributed by the National Transportation Safety Board to one form of low altitude wind shear–the microburst [1]–with associated loss of 438 lives. The U.S. Federal Aviation Administration (FAA) is in the process of deploying 45 Terminal Doppler Weather Radars (TDWR) [2] that will automatically detect hazardous wind shear conditions at large airports. Deployment of TDWRs at smaller airports, and in locales where thunderstorm activity is infrequent, is not cost beneficial, however, owing to the high procurement and life-cycle operation costs of this radar.

FAA-sponsored research and field demonstrations have shown that current generation terminal air-traffic control radars or Airport Surveillance Radars (ASR-8 and ASR-9) could also provide for detection of low-altitude wind shear through the addition of a parallel data processing chain for estimation of Doppler winds and automated wind shear signature detection [3]. Life cycle costs of this ASR Wind Shear Processor (WSP) are significantly less than those of the dedicated TDWR, thereby justifying its procurement for approximately 35 additional airports. An FAA acquisition program for the WSP is underway with operational deployment targeted for circa year 2000.

Using internal research and development resources, the UNISYS Corporation has recently developed a Microburst Prediction Radar (MBPR) to provide detection and short-term predictions of the most hazardous form of low altitude wind shear in the vicinity of an airport [4]. The MBPR is intended for deployment on- or near-airport so as to minimize range coverage (and associated radar power-aperture) requirements. Like the ASR-WSP, the cost of MBPR is significantly less than that of the TDWR so that its deployment at smaller airports might be economically justified if performance is operationally acceptable. Field tests of engineering prototypes of the MBPR have been conducted in conjunction with FAA-sponsored TDWR and WSP demonstration programs.

In this paper, we assess the capabilities and limitations of each of these systems using a consistent methodology that emphasizes comparative analysis of the significant parameters of each radar in relation to wind shear phenomenology. An extensive data base on wind shear event radar cross section, spatial structure and intensity distribution–derived through our FAA-sponsored testing of TDWR and ASR-WSP prototypes–is an important asset in developing this comparison. The following issues are considered:

(i) Radar sensitivity;
(ii) Ground clutter rejection capability;
(iii) Radar elevation beamwidth and its effect on the capability to accurately measure low-altitude wind shear;
(iv) Obscuration within the coverage area of operational concern due to weather returns from beyond the radar's unambiguous range;
(v) Obscuration due to path length attenuation ("shadowing");
(vi) Effects of radar siting on the ability to accurately measure the operationally important along-flight-track component of the wind shear.

In support of these analyses, we summarize field test data available for each system and attempt to reconcile resulting skill measurements (probability of wind shear event detection, probability of false alarm) with the above.

Section 2 provides an overview of thunderstorm generated low altitude wind shear, with emphasis on features that are significant for radar detection of the phenomena. In section 3, we summarize the important parameters of each of the above wind shear detection systems. These results are combined in Section 4 to address the issues delineated in the previous paragraph. Field test results are discussed in Section 5.

2. Microburst Phenomena

As illustrated in Figure 1, *microbursts* are small scale thunderstorm downdrafts that produce a highly divergent horizontal wind pattern at the surface that is roughly radially symmetric about the downdraft axis. Penetrating aircraft encounter, in rapid succession, increased headwind followed by performance-reducing downdraft and tailwind. Figure 2, compiled from field measurements with the FAA/Lincoln Laboratory TDWR testbed, shows distributions of peak measured radial velocity differential across microbursts. These are approximately exponential in shape; although 80% of the microbursts exhibited peak differential velocities of less than 20 m/s, events with differential velocities of approximately 50 m/s have been observed.

* This work was sponsored by the Federal Aviation Administration. The views expressed are those of the authors and do not reflect the official policy or position of the U.S. Government.
‡ Opinions, interpretations, conclusions, and recommendations are those of the authors and are not necessarily endorsed by the United States Air Force.

0-7803-2120-0/95/0000-0486 $4.00 © (1995 IEEE)

Figure 3 plots cumulative distributions of the meteorological "radar reflectivity factor" {10 log [Z (mm^6/m^3)]–see [5]} at the surface in the region of maximum horizontal outflow velocity. Qualitatively, reflectivity factors less than about 15 dBz are associated with clear-air scattering; 30 dBz corresponds to mist or light rain and 40 dBz is moderate to heavy rain. Although most southeastern U.S. microbursts exhibit high radar reflectivities in the rain shafts associated with their downdraft cores, 20% of the Orlando microbursts tabulated in Figure 3 exhibit peak reflectivities at the outflow maximum velocity volume of 30 dBz or less. Radar reflectivities in midwestern and, particularly, high-plains (i.e., Denver) microbursts are lower. For example, the median reflectivity factor in the outflows of Denver microbursts is only 10 dBz.

The divergent, horizontal outflow winds associated with microbursts are confined to a shallow layer near the Earth's surface. Comparison of field measurements with theory and laboratory studies indicates that a "wall-jet" model is a useful first approximation to the distribution of microburst winds with height. With this model, the outflow velocity peaks within approximately 100 m of the surface and decreases above this level roughly linearly:

$$(1) \qquad V(Z) = 1.13\, V_p \{ 1 - 0.56\, Z/Y \}$$

Here V(Z) is outflow wind magnitude at altitude Z and V_p is the peak wind magnitude. The parameter Y is readily seen be the altitude at which the outflow's horizontal winds fall to one-half their peak value. Median values for the outflow "half-height", Y, have been reported to be 400 m for microbursts in Huntsville, Al. [6] and 600 m for microbursts in Denver [7]. Figure 4 is a distribution of microburst half-heights measured by the FAA/Lincoln Laboratory TDWR testbed using range-height indicator (RHI) scans for microbursts at ranges less than 10 km; with the radar's 1 degree beam this translated to vertical resolution of 180 meters or less.

3. Wind Shear Detection Radars

Parameters of the three radars are compared in Table 1. The TDWR has in general been optimized for measurement of low altitude wind shear phenomena. Power-aperture product are sufficient for measurement of essentially all convective-related wind shear phenomena, even those that occur in the absence of significant precipitation at the surface. Its narrow pencil beam supports radial wind measurement within the lowest few hundred meters of the atmosphere while avoiding main-lobe illumination of ground scatterers. A TDWR is sited, where possible, to look along an airport's principal runways so that the radial wind measurements will reflect the operationally important headwind-tailwind shear component. The only significant deficiencies in TDWR weather surveillance capabilities occur as a result of its operation at C-band. (Frequency authorization at S-band was not possible owing to interference considerations involving FAA ASRs and National Weather Service Weather Surveillance Radars.) Operation at C-band is more stressing from the viewpoint of range-Doppler ambiguity resolution, and may result in significant path-length attenuation, or "shadowing." The latter effect may bias reflectivity estimates for precipitation echoes that are behind intense intervening precipitation.

Airport Surveillance Radars are designed primarily to provide detection and tracking of skin-echoes from aircraft to a range of 60 nmi and an altitude of at least 20,000 feet. An ASR's transmitted frequency, power, pulse-to-pulse stability and receiver sensitivity are well suited for weather sensing. Conversely, its broad elevation beamwidth, rapid antenna scan rate and non-uniform pulse-repetition frequency introduce significant complications for the quantitative measurement of low-altitude wind shear phenomena. In particular, reduced antenna gain makes detection of very low radar cross section wind shear events problematic, and the corresponding broad elevation beam introduces an interfering signal component associated with precipitation echoes above the near-surface layer of outflow winds (see Figure 1). Reference [8] in these conference proceedings describes the issues and necessary data processing for achieving an operationally useful wind shear detection capability with this radar.

UNISYS' Microburst Prediction Radar (MBPR) has as performance goals detection and prediction of microbursts within 10 km of the radar. System size and costs are minimized by operation at X-band and the choice to provide coverage only in the vicinity of the airport. A very low energy pulse is used, resulting in low single-pulse signal-to-noise ratio (SNR) for many weather echoes of operational concern. A high pulse-repetition frequency provides long (approximately 1500 sample) CPIs to facilitate Doppler estimation at low SNR. The associated unambiguous range (18 km) is very small however, and may result in significant interference from out-of-trip weather and ground clutter. Like the ASR-WSP, the MPR utilizes a broad elevation beam for detection of wind shear at the surface and must therefore contend with main-lobe ground clutter illumination and interference from precipitation echoes entering the beam from above thunderstorm outflows. Path-length attenuation for transmission through intervening precipitation at X-band is a significant issue.

4. Performance Analyses

This section compares the capabilities of the three wind shear detection systems based on:

(i) The radars' parameters;
(ii) A common data base of relevant wind shear event characteristics (e.g., radar reflectivity, outflow height, peak winds, storm spatial distributions) and representative ground clutter backgrounds.

4.1 Radar Sensitivity

The parameters in Table 1, and the meteorological form of the radar range equation can be used to derive the sensitivity of each of these radars to meteorological echoes. For the TDWR, a beamfilling meteorological target with reflectivity factor equal to -10 dBz would produce a single-pulse signal-to-noise ratio (SNR) of 7 dB at a range of 30 km. This SNR would decrease with increasing range according to a range-squared law, assuming that no range varying receiver gain is employed. On a relative basis, the ASR-9 and MBPR provide respectively 19 and 42 dB less SNR than the TDWR on a single-pulse basis; this deficit is compounded by any "beamfilling losses" that result when a near-surface wind shear pattern subtends an angle significantly less than that of the broad elevation beams of these two radars. For example, beamfilling loss for a 300 m

deep outflow at a range of 10 km from these radars would be 5 dB (15 dB) for the ASR-9's low (high) elevation beams and 3 dB for MBPR's horizon beam.

Table 1.
Comparative Radar Parameters

	TDWR	ASR-9	MBPR
Transmitted Frequency	5.6 GHz	2.8 GHz	10 GHz
Peak Power	250 KW	1100 KW	0.08 KW
Pulse Width	1.1 microsecond	1 microsecond	1.25 microsecond
Pulse Repetition Frequency	300 sec $^{-1}$ (long range surveillance tilts) 1200-1700 sec $^{-1}$ (Doppler velocity tilts)	900-1200 sec $^{-1}$ (avg) Alternates between two PRFs every 8-10 pulses	8333 sec $^{-1}$
Azimuth, Elevation Beamwidths	0.5 degree	1.4 degree (az) 5 degree (elevation)	3.2 degree (surface beam)
Antenna Gain	51 dB	34 dB	35 dB (surface beam)
Antenna Scan Rate	25 degrees/sec	75 degrees/sec	18 degrees/sec
Nominal Coherent Processing Interval	60 pulses	20 pulses	1500 pulses
Siting	5 to 15 km off-airport	on-airport	on-airport
Scan Pattern	16 elevation tilts encompassing 120 degree sector centered on airport. 2,5 minute volume scan period with near-surface wind shear detection scans once per minute.	two ("low" and "high") overlapped elevation beams scanned in azimuth only. Beam "noses" at 2° and 5.5°. 5 second scan period.	Surface beam plus six overlapped beam-pairs directed aloft. Scanning in azimuth only. 20 second scan period.

As shown in Table 1, these radars employ very different coherent processing intervals, pulse repetition frequencies and wavelengths, all of which enter into the velocity estimate accuracy that is achievable at a given SNR. As a "normalizing" factor, we employ equation (6.26) in [9]–an expression for mean Doppler estimate variance that depends on CPI length, weather signal spectrum width, weather signal to noise ratio, radar wavelength and pulse repetition frequency–to compute the single pulse SNR at which a Doppler estimate variance of 1 m/s is achievable. Weather spectrum width of 3 m/s is assumed. For the TDWR and ASR-9 parameters, single-pulse SNR of about 6 dB is required. Owing to its relatively large Nyquist interval (i.e., smaller relative signal spectrum width) and long CPI, this equation implies that MBPR can achieve 1 m/s variance at an SNR of -1 dB. We note that in a technical report submitted to the FAA [10], UNISYS shows results from Monte Carlo simulations employing a proprietary "poly-pulse pair algorithm" that suggest that Doppler estimate variance can be maintained below 1 m/s at SNRs of less than - 8 dB.

Range dependent sensitivity limits–derived from the above arguments–can be convolved with measured distributions of microburst reflectivities (e.g., Figure 3) to calculate a range-averaged measure of the fraction of wind shear events that would exceed the SNR requirement of each of the three radars. This fraction is given by:

$$(2)\quad F_{SNR}=\frac{1}{R_{max}-R_{min}}\int_{R_{min}}^{R_{max}}\int_{Z_N(R)+BL(R)+T_W}^{\infty} p(Z_W)\,dZ_W\,dR$$

Here R_{min} and R_{max}, the range limits of operational concern for wind shear detection, are taken as 5 and 25 km respectively for the off-airport TDWR, and 0 and 10 km respectively for the on-airport ASR-9 and MBPR. $Z_N(R)$ is the system noise equivalent weather reflectivity, BL(R) is beamfilling loss and T_W is the SNR requirement for accurate velocity measurement, chosen using the arguments of the preceding paragraph. $P(Z_W)$ is the probability density function for the wind shear type/environment under consideration. Table 2 lists values for this fractional visibility for the three radars using the Orlando and Denver microburst "outflow peak" reflectivity distributions shown in Figure 3. For MBPR, we consider both the -1 dB SNR threshold as calculated according to the previous paragraph, and a -10 dB threshold suggested by the UNISYS report [10]. In the southeastern U.S. environment where microburst outflows are characterized by relatively high radar cross sections, system noise is not a significant factor for any of these systems. In an environment subject to frequent "dry" microburst activity such as Denver, the ASR-9 and MBPR systems will experience a significant loss in capability for microburst detection under noise limited conditions, relative to the TDWR.

Table 2.
Range Averaged Fractional Visibility as Defined By Equation 2

	Denver Outflow	Orlando Outflow
TDWR	0.88	1.00
ASR-9	0.72	0.99
MBPR (-1 dB SNR Threshold)	0.42	0.94
MBPR (-10 dB SNR Threshold)	0.64	0.98

4.2 Ground Clutter

Analyses similar to the above can be used to assess the impact of ground clutter residue on the wind shear detection capability of these radars. As a common ground clutter data base, we use measurements of ground clutter obtained in moderate (Orlando, FL) and severe (Albuquerque, NM) clutter environment using the FAA/Lincoln Laboratory transportable ASR-9 testbed facility. The measured intensity distributions, scaled in terms of the equivalent weather reflectivity factor, are shown in Figure 5. We will assume that each of the radars' transmitter/receiver chains are sufficiently stable to support 50 dB suppression of the ground clutter returns through the use of high pass notch filters. This value is used for the clutter suppression capability of both the ASR-9 and the MBPR since both radars have similar gains (relative to the "nose" of their beams) on the horizon. For the TDWR, we assume an additional 24 dB clutter suppression to account for:

(i) The different antenna pattern. For a TDWR scanning at a 0.3 degree elevation angle , the two-way antenna gain for ground scatterers will be down, on average, roughly 10 dB;

(ii) The greater average range from the TDWR to the area of operational concern. Assuming that the predominant ground scatterers are large in extent relative to the pulse resolution volume, the ground clutter will fall off as $(1/\text{range}^3)$ versus $(1/\text{range}^2)$ for beamfilling weather echoes. This produces, on average, an additional 14 dB lowering of the relative equivalent weather reflectivity of the ground clutter as viewed by the TDWR.

Given $p(Z_C)$, the density function for the ground clutter equivalent weather reflectivity, then the range averaged fraction of wind shear events that is not obscured by clutter residue can be calculated as:

$$(3)\quad F_C = \int_0^{\infty} p(Z_C) \int_{Z_c - S + T_c}^{\infty} p(Z_W)\, dZ_C\, dZ_W$$

Here S is the clutter suppression capability of the radar and T_C is the required weather-to-clutter residue power ratio. We shall take this threshold as 10 dB for each of the radars. The weather reflectivity density distributions are taken from Figure 3 as before. Table 3 lists this fractional wind shear event visibility for the Denver and Orlando microburst outflow distributions, calculated for both the moderate (Orlando) and severe (Albuquerque) clutter environments.

Table 3.
Fractional Visibility of Wind Shear Events in the Presence of Representative Ground Clutter. See Equation 3.

	Mod. Clutter	Orlando	Severe Clutter	Albu-querque
	Denver Outflow	Orlando Outflow	Denver Outflow	Orlando Outflow
TDWR	0.99	1.00	0.97	1.00
ASR-9	0.85	0.98	0.75	0.96
MBPR	0.89	0.99	0.81	0.98

For the weather and clutter distributions used here, the calculation shows small impact on TDWR microburst detection. Against the lower cross section Denver outflows, both the ASR-9 and MBPR would experience more substantial microburst obscuration due to clutter residue, particularly when the clutter environment is severe. The slightly greater obscuration calculated for the ASR-9 is the result of larger assumed beamfilling loss relative to MBPR.

4.3 Precipitation Echoes above the Outflow:

The wall jet model of equation (1) implies a roughly linear decrease in microburst outflow speed with altitude above the level of maximum wind. In this case, if precipitation reflectivity is constant with altitude, the mean velocity measured by a radar with a symmetric elevation beam will be equal to the actual velocity at the height of the middle of the beam. (For simplicity, we ignore a very shallow layer near the surface where wall jet velocity increases with height.) Both TDWR and MBPR employ symmetric elevation beams with respective beam centers typically at 0.3^o and 1.6^o. Although the ASR-9's elevation beam is cosecant-squared, the "difference pattern" that corresponds to the dual-beam velocity estimator used by the ASR-WSP [8] can be shown to be equivalent to a narrower, symmetric beam centered at 1.3^o under the above assumptions on microburst reflectivity and outflow speed variation with height.

Probability densities of hazardous microburst peak differential velocities (Figure 2) can be roughly fit be an exponential function of the form:

$$(4)\quad p(\Delta V_p) = \exp(-0.18\Delta V_p) / \exp(-0.18 * \Delta V_{hazard})$$

The factor ΔV_{hazard} in equation (4) is the threshold at which the differential velocity across a microburst outflow becomes a significant hazard to an aircraft. We shall define a beam-shape induced missed detection as occurring when a radar's elevation beam pattern causes the reported velocity differential for a microburst with actual ΔV_p greater than ΔV_{hazard} to fall below ΔV_{alert}, the threshold for issuing an alert. Operational procedures for ground based wind shear detection systems have generally set ΔV_{hazard} and ΔV_{alert} at 15 m/s and 10 m/s respectively. The probability for a beam shape induced miss is:

$$(5)\quad P_{miss} = \int_{\Delta V_{hazard}}^{\infty} p(V_p)\,dV_p \qquad \int_{0}^{Ycritical(Vp)} p(Y)\,dY$$

For a beam-center height, Z_{beam}, the wall jet model of equation (1) has been used to define the critical outflow "half-height," $Y_{critical}$, below which the outflow differential velocity will be reported as being less than V_{alert}:

$$(6)\quad Y_{critical}(Vp) = \frac{Z_{beam}}{1.8 - 1.6 \times V_{alert} / V_p}$$

The measurements shown in Figure 4 are used to derive a representative density function of microburst half-heights, p(Y).

Table 4 lists the complement of P_{miss}–the associated "detection probability" with respect to beam shape induced velocity estimate biases–for each of the three radars. P_{miss} has been averaged over the areas of operational coverage for each radar in order to account for the variation of beam-center height with range.

Table 4.
Detection Probability for Microbursts with Respect to Beam-Shape Induced Velocity Estimate Biases. See Equations (5) and (6).

	$1-P_{miss}$ ΔV_{hazard} = 15 m/s ΔV_{alert} = 10 m/s
TDWR	1.00
ASR-9	0.95
MBPR	0.87
MBPR (with ΔV correction: Y=325m)	0.97 (P_{fa} =0.19)
MBPR (with ΔV correction: Y=400m)	0.95 (P_{fa} = 0.05)

In practice, the MBPR applies a static, range dependent correction factor to its measured differential velocities to account for the downward bias introduced by its relatively broad surface beam. While this will boost the "detection" probability calculated above (effectively the alert threshold, ΔV_{alert}, in equation (6) is scaled down), it will also introduce "false alerts" when reported differential velocities for relatively deep, weak intensity outflows are scaled above this threshold. Figure 6–a microburst case study from an ongoing FAA-sponsored evaluation of MBPR in Memphis–illustrates the potential for this ΔV correction to result in an overestimate of the actual differential velocity associated with a microburst. In the last two rows of Table 4, $1-P_{miss}$ is recalculated for MBPR assuming correction factors appropriate for 325m and 400 m deep outflows–respectively, the median and average outflow heights in Figure 4. The corresponding "false alert" probability, P_{fa}, has been calculated in a fashion analogous to equations (5) and (6). In the table, P_{fa} is the ratio of the number of "alerts" generated by outflows with true differential velocity less than ΔV_{alert} to the number of actual hazardous outflows (i.e., differential velocity greater than ΔV_{hazard}). These calculations indicate that while MBPR's ΔV correction may be quite effective in boosting detection probability, the associated false alert probability is sensitive to the choice of correction factor in relation to the actual distribution of microburst outflow heights.

4.4 Weather Echoes from Beyond the Unambiguous Range

We calculated typical levels of "out of trip" weather obscuration for the three radars using measurements from the National Weather Service WSR-88D at Memphis, TN. The WSR-88D provides range-unambiguous reflectivity measurements to 460 km, well beyond the unambiguous ranges of any of the radars considered here. For this study, three 2.5 to 3 hour weather episodes were analyzed. Two consisted of scattered, wide spread "air mass" thunderstorm activity, and the third involved an organized line storm traversing the radar coverage region. These are representative of situations that may be associated with hazardous microbursts.

For each of the three radars, WSR-88D echoes were artificially folded back into the first trip. Power corrections were applied to account for echo true range and vertical extent relative to the wind shear detection radars' beam patterns. As a function of assumed first-trip weather reflectivity, Figure 7 shows for the three radars the fractional area within their operational coverage regions where out of trip weather returns would be within a 5 dB signal-to-interference limit assumed necessary for accurate velocity estimation. These fractional areas have been averaged over the three weather episodes and the 25 to 30 WSR-88D volume scans performed during each episode.

As would be expected, fractional obscuration is largest for the MBPR with its very high PRF. Microbursts with reflectivity of 20 dBz would, on average, have been overlayed by significant out-of-trip returns over 5% of the 0-10 km region of operational concern. Least obscuration occurs using the ASR-9's long PRF and relatively low gain antenna.

A "detection probability" with respect to range-folded echo interference can be estimated using the curves of Figure 7, $f_{obsc}(Z_W)$, and the microburst reflectivity factor densities, $p(Z_W)$, corresponding to Figure 3:

$$(7)\quad 1 - P_{obscuration} = 1 - \int_{0}^{\infty} p(Z_W) f_{obsc}(Z_W)\,dZ_W$$

As before, the variable Z_W is the weather reflectivity factor. Table 6 lists this probability that range ambiguous weather echoes will not obscure microburst echoes for the Memphis data set analyzed.

Table 5.
Detection Probabilities for Microbursts as Affected by Range Ambiguous Weather Echoes. See Equation (7).

	1- $P_{obscuration}$ (Denver Outflow)	1-$P_{obscuration}$ (Orlando Outflow)
TDWR	0.96	1.00
ASR-9	1.00	1.00
MBPR	0.92	0.99

4.5 Asymmetric Microburst Outflows

Actual microburst outflow wind speeds may vary with aspect angle. In this scenario, a Doppler radar's measurement of the radial wind component will not accurately reflect aircraft headwind-tailwind wind shear unless the radar beam is aligned with the flight path. In general, it is more difficult to approximate such alignment over the entire "arena" of operational concern–runways and approximately 3 nmi final approach/initial departure corridors–for a radar that is sited near or within the runway complex. This circumstance places the on-airport ASR-9 and MBPR at a disadvantage relative to the off-airport TDWR with respect to accurate quantification of microburst hazard level.

Hallowell [11] analyzed microburst vector wind fields retrieved from multiple Doppler weather radar measurements to characterize asymmetry, both with respect to areal extent and outflow wind strength. He found median maximum to minimum outflow differential velocities ratios of 1.9. For random outflow orientations, this translates to an average underestimate of outflow maximum strength by 30%. The impact on the accuracy of reported shear relative to actual runway-oriented headwind tailwind shear will of course be dependent on the specifics of the runway and radar placements, the orientation of the microburst's maximum strength axis and the asymmetry ratio.

4.6 Path Length Attenuation (Shadowing)

At wavelengths less than 10 cm, Mie scattering and absorption of electromagnetic energy along the two-way path to a radar's measurement volume may be significant. Battan [5], (Table 6.3) lists formulae for attenuation coefficients versus radar reflectivity at various radar wavelengths. For reflectivity factors of 50, 55 and 60 dBz, these evaluate respectively to 1.2, 2.6 and 6.1 dB/km at the MBPR's 3 cm operating wavelength, and 0.1, 0.3 and 0.6 dB/km at the 5 cm operating frequency of TDWR. Two-way path length attenuation for MBPR through a 50 dBz rain echo extending over its operational coverage region would be as large as 24 dB, clearly significant relative to its SNR margin with respect to typical wind shear event reflectivities. For the TDWR, the issue is not acute for Doppler velocity measurement, even under extreme assumptions. Intense 55 dBz rain over the entire path to a wind shear target at 25 km would produce two-way attenuation of only 15 dB. At this range, the attenuated echo from a very dry 3 dBz microburst would still produce adequate SNR (6 dB) for the TDWR to accurately measure its velocity.

4.7 Composite "Detection" Probabilities

If we assume that the "miss mechanisms" discussed above are largely independent, then the "detection probabilities" derived in Sections 4.1 through 4.4 can be multiplied to provide an overall measure of the relative capabilities of the three radars for microburst detection. These are listed in Table 6 for "favorable" and "challenging" assumptions. "Favorable" assumptions include wind shear reflectivity distributions represented by the high radar cross section Orlando data set in Figure 3 and a moderate clutter environment ("Orlando", Figure 5). "Challenging" assumptions involve microburst reflectivity distributions with a significant probability of "dry" outflows ("Denver," Figure 3) and severe ground clutter ("Albuquerque," Figure 5). For MBPR, composite "detection probabilities" are shown with both -1 and -10 dB SNR thresholds (see Section 4.1) and both with and without the ΔV correction discussed in Section 4.3. As discussed in those sections, the authors do not at this writing have sufficient information to reliably assess whether or not the more optimistic assumptions are justified.

Table 6.
Composite "Detection Probabilities"

	Overall Pd ("Favorable")	Overall Pd ("Challenging")
TDWR	1.00	0.82
ASR-9	0.92	0.51
MBPR (-1 dB SNR limit. No ΔV correction)	0.80	0.27
MBPR (-10 dB SNR limit. ΔV correction)	0.91	0.45

These numbers should not be interpreted literally as actual microburst event detection probabilities. Our fractional obscurations have been calculated on a pixel by pixel basis and do not consider the distributed nature of both the meteorological targets and the interferers. Discrete clutter sources for example, while extremely strong, may have no significant impact on detection capability when they obscure only a very small area of a microburst's Doppler velocity signature. Further, the reflectivity of actual microbursts varies significantly not only from event to event, but across the extent of an individual outflow. Thus, even if velocities in the lower reflectivity "outflow" considered in our analysis are not measurable, a radar may still detect the presence of microburst wind shear closer to the downdraft core, *albeit* with a potential downwards bias in its estimate of the associated differential velocity.

5. Field Evaluations

Table 7 lists field measurements of microburst detection and false alert probabilities for each radar, broken out into "dry" and "moist" wind shear environments as represented by the Denver and Orlando reflectivity distributions in this report. The TDWR and ASR-WSP results are from FAA-sponsored field performance trials of prototype systems [12,13] that have been conducted each of the last eight years at different U.S. sites. These detection and false alert "scores" represent a scan-by-scan comparison of microburst reports generated by the

respective radars' automatic wind shear detection algorithms to "truth"–microbursts delineated by manual examination of the best available data on the occurrence of low altitude wind shear. In the case of TDWR, this has usually been taken as the TDWR low altitude Doppler velocity and reflectivity imagery. For ASR-WSP, independent data from co-located pencil beam Doppler weather radars has been used in generating the "truth" data set. The probability of detection, P_d, is the number of detected microbursts divided by the total number of microbursts. The probability of false alert P_{fa} is the number of algorithm alarms not associated with valid microbursts divided by the total number of alarms issued by the algorithm.

Table 7.
Detection and False Alert Probabilities from Field Measurements

	"Dry" Environments		Moist Environments	
	Location-Years	**Average P_d and P_{fa}**	**Location-Years**	**Average P_d and P_{fa}**
TDWR	Denver - '87,'88	P_d 0.98 P_{fa} 0.04	Orlando - '90-'92	P_d 0.99 P_{fa} 0.03
ASR-9 WSP	Albuquerque - '93,'94	P_d 0.78 P_{fa} 0.12	Orlando - '90-'92	P_d 0.97 P_{fa} 0.09
MBPR	Denver - '91	P_d not P_{fa} available	Orlando - '92 (Unisys)	P_d 1.00 P_{fa} 0.01
			Orlando - '92 (Lincoln Labs)	P_d 0.77 P_{fa} 0.08

A more limited evaluation set for the MBPR is available to us, based on measurements in coincidence with FAA-supported activities in Denver, CO, Orlando, FL, and Memphis, TN. The first Orlando entry is taken from Unisys' report to the FAA [10]. Our understanding is that methodology equivalent to that described in the preceding paragraph was used to score MBPR alerts with respect to the automated output of the TDWR prototype being operated for the FAA by Lincoln Laboratory. The second Orlando entry is from a very limited "independent" evaluation performed by one of the authors. MBRP microburst reports from three storm days representative of Orlando thunderstorms were scored against manually generated "truth" that was derived from the Lincoln Laboratory TDWR testbed and other Doppler weather radars operating in the area. Subsequent to the analysis, we learned from Unisys that the MBPR alerts that were scored were an intermediate product, generated prior to application of the ΔV correction discussed in section 4.3. Thus these last results should be considered with reference to the "uncorrected" performance estimates (e.g., third row of Table 4) in Section 4.3.

We note that the ground clutter environments against which these radars operated were relatively mild in Orlando. The clutter was significantly more intense in Denver and particularly Albuquerque. (Albuquerque's median clutter equivalent weather reflectivity was roughly 10 dB higher than Orlando.)

Qualitatively, the results for the TDWR and the ASR-9 WSP track the analyses of Section 4. WSP results from the relatively benign Orlando environment are quite credible in relation to the TDWR, although a three-fold higher false alert probability has been allowed in order to maintain near-unity detection probability for hazardous microbursts. The non-optimized parameters of the ASR-9 preclude maintaining this level of performance in the face of the severe ground clutter and low radar cross section microbursts encountered in the Albuquerque environment. Consistent with the analyses of Section 4, a significant drop in detection probability occurs: case studies indicate that a major portion of the misses occur under conditions of unfavorable weather signal to clutter residue or noise.

Lincoln Laboratory's (unintentional) analysis of MBPR microburst alerts prior to application of the ΔV correction is probably a major contributor to the discrepancy relative to Unisys' analysis of Orlando performance. Section 4.3 indicates that significant increases in P_d may be achieved with the ΔV correction. It is surprising however, that perfect detection is achieved even with the correction and more so that the false alert probability reported by Unisys remains negligible after application of this unbiasing factor. Although MBPR was operated in 1991 in Denver, this was a "proof of concept" exercise that did not, to our knowledge, include quantitative performance analysis.

6. Summary and Discussion

Our analyses indicate that any of these radar systems can provide credible detection of microburst phenomena under favorable conditions where microburst reflectivities are high relative to interference from system noise, ground clutter residue and out of trip weather. The decidedly sub-optimal parameters of the lower cost ASR-9 WSP and MBPR systems will result in more rapid degradation of performance as the intensity of one or more of these interferers increases. Microburst detection performance of the lower cost WSP and MBPR systems appear approximately equivalent given:

(i) Favorable assumptions on the efficacy of Unisys-proprietary algorithms for low-SNR velocity estimation and beam-shape compensation;
(ii) The absence of severe attenuation conditions or out-of-trip weather that is significantly more intense than that in the three data sets we analyzed.

To the extent that these conditions are not met, the ASR-9 WSP would appear to have a significant advantage owing to higher power-aperture product, longer unambiguous range and split-elevation-beam processing to achieve vertical resolution.

As of this writing, deployment of operational TDWRs is well underway. Several sites are already commissioned and FAA schedules call for deployment to be completed in 1996. Testing and refinement of an ASR-9 WSP functional prototype are continuing, and current FAA acquisition plans would result in this system being fielded nationally early in the next decade. The FAA will support Unisys in continued testing of the MBPR at Memphis this summer, using data from other nearby meteorological sensors (Doppler radar, surface stations) as ground truth. Independent evaluation of data from this test should further clarify MBPR's microburst detection capability, at least for a moist wind shear environment.

References:

(1) Fujita, T.T., *The Downburst*, SMRP Research Paper 210, University of Chicago, 1985.

(2) Michelson, M., W.W. Shrader and J.G.Weiler, "Terminal Doppler Weather Radar," Microwave Journal, Horizon House Inc. Vol. 33, No. 2, 139-148.

(3) Weber, M.E. and M.L. Stone, "Low Altitude Wind Shear Detection Using Airport Surveillance Radars," Conference Proceedings, IEEE 1994 National Radar Conference, Atlanta, Ga., 29-31 March, 1994.

(4) Rubin, W.L., C.H. Leyh and J.J. Owenburg, "A Low Cost Weather Radar for Airports," Preprints: 26th International Conference on Radar Meteorology, Norman Oklahoma, 24-28 May 1993, AMS.

(5) Battan, L.J., *Radar Observation of the Atmosphere*, University of Chicago Press, 324 pp, 1973.

(6) Biron, P.J. and M.A. Isaminger, "High Resolution Microburst Outflow Vertical Profile Data from Huntsville, AL and Denver, CO," Lincoln Laboratory Project Report ATC-163, FAA-PS-88-17, 1991.

(7) Wilson, J.W., R.D. Roberts, C. Kessinger and J. McCarthy, "Microburst Wind Structure and Evaluation of Doppler Radar for Airport Wind Shear Detection," J. Climate Appl. Meteor., 23, 898-914, 1984.

(8) Weber, M.E., R.L. Delanoy and E.S. Chornoboy, "Data Processing Techniques For Airport Surveillance Radar Weather Sensing," Conference Proceedings, IEEE 1995 International Radar Conference.

(9) Doviak, R.J. and D.S. Zrnic, *Doppler Radar and Weather Observations*, Academic Press, 458 pp., 1984.

(10) "Validation Test of Microburst Prediction Radar: Final Report," Contract DTFA01-C-00054, June 1993.

[11] Hallowell, R.G., "Aspect Angle Dependence of Outflow Strength in Denver Microbursts: Spatial and Temporal Variations," Preprint Volume: 16th Conference on Severe Local Storms, Oct. 22-26, 1990, Kananaskis Park, Alta., Canada. Published by AMS.

(12) Bernella, D.M., "Terminal Doppler Weather Radar Operational Test and Evaluation - Orlando, 1990," Lincoln Laboratory Project Report ATC-179, FAA-NR-91-2, 1991.

(13) Weber, M.E., "Airport Surveillance Radar (ASR-9) Wind Shear Processor: 1991 Test at Orlando, FlL," Lincoln Laboratory Project Report ATC-189, FAA-NR-92-7, 1992.

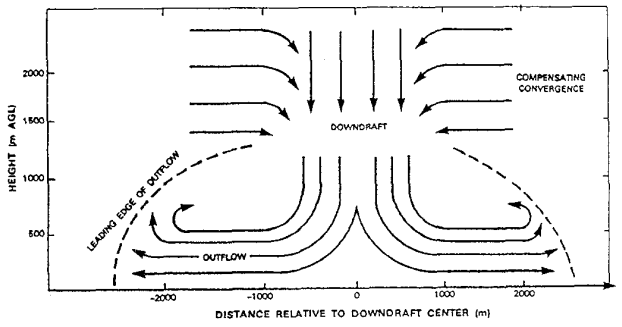

Figure 1. Vertical cross section of microburst wind structure.

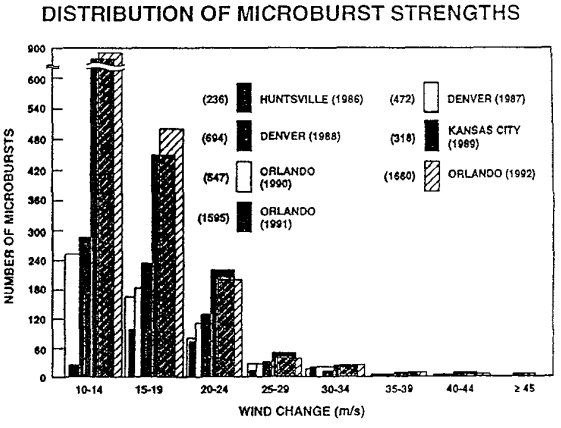

Figure 2. Density function for microburst differential velocities. Data are from FAA/Lincoln Laboratory TDWR testbed.

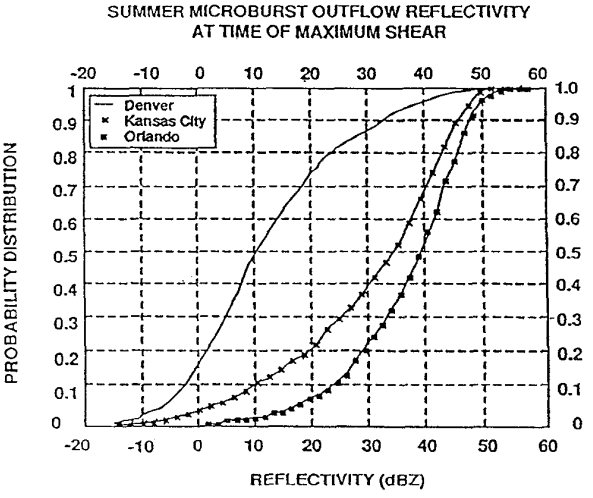

Figure 3. Distribution of the radar reflectivity factor for the points of maximum approaching and receding radial velocity in Orlando, Kansas City and Denver microbursts. This "outflow velocity core" is often displaced from the higher reflectivity rain shaft that generates the outflow.

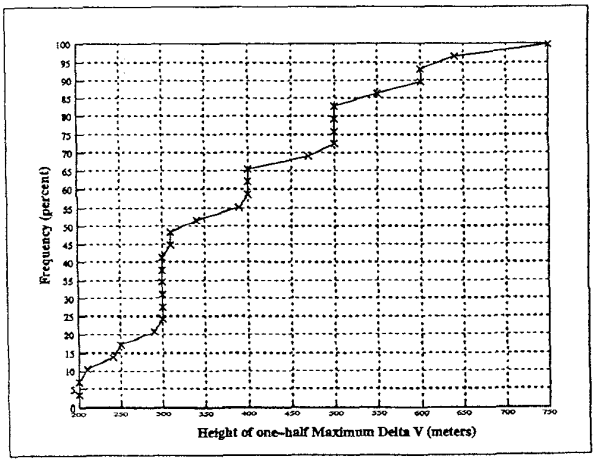

Figure 4. Distribution of the "half-height" of microburst outflows measured in Orlando.

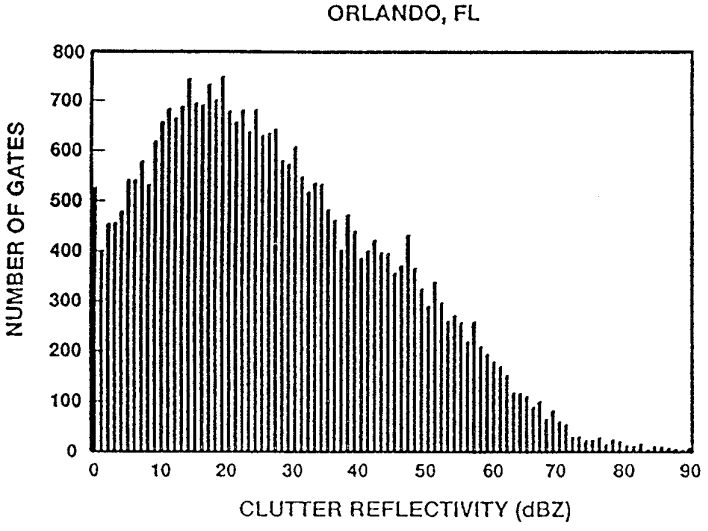

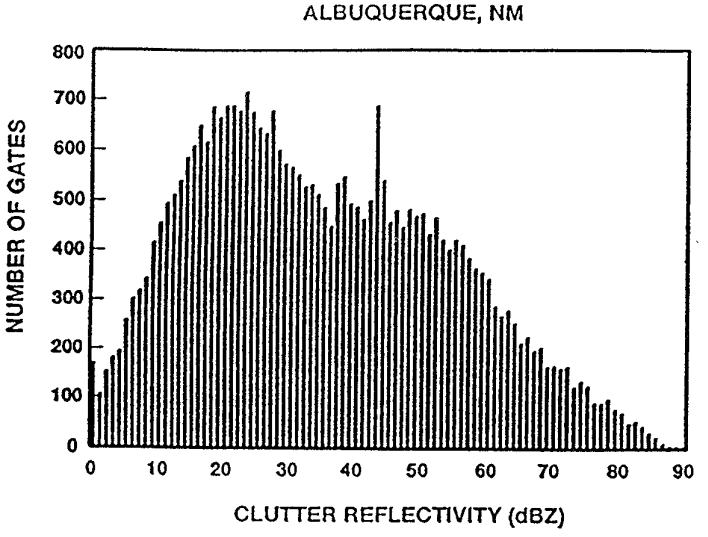

Figure 5. Density function for ground clutter measured by FAA/Lincoln Laboratory ASR-9 testbed in Orlando and Albuquerque. Clutter returns are scaled in terms of equivalent weather reflectivity factor.

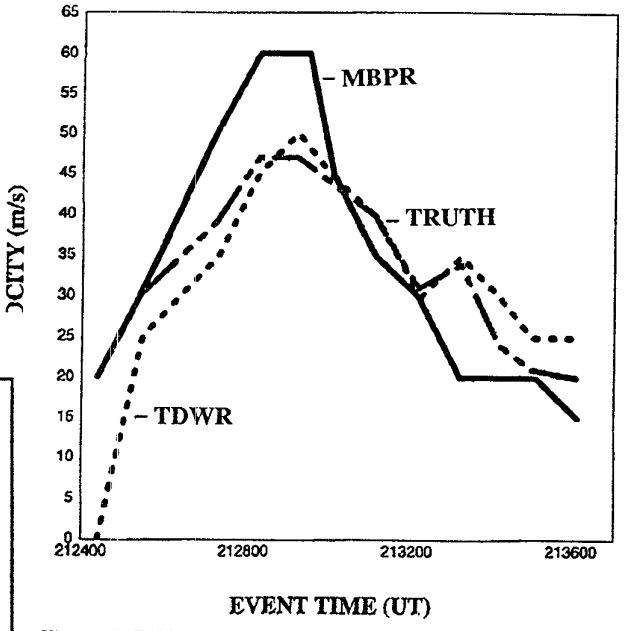

Figure 6. Differential velocity versus time as measured by TDWR and MBPR during a microburst near the Memphis airport. The "truth" curve represents a human analyst's best interpretation of the actual time-evolution of this microburst. Data are from an ongoing FAA-sponsored evaluation of MBPR.

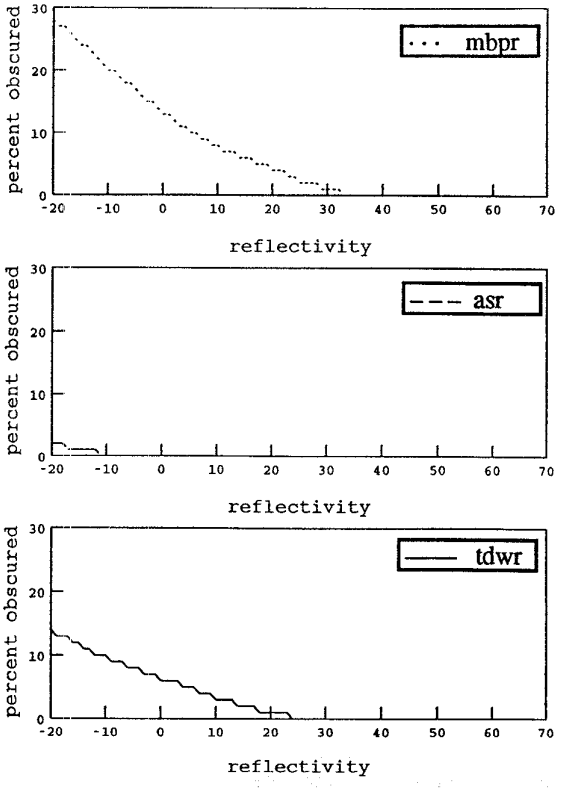

Figure 7. Percent obscuration by range-ambiguous weather echoes within the respective areas of operational concern of MBPR, ASR-WSP and TDWR.